Advanced Airfoil Design for General Aviation Propellers

Frank Taverna*
Grumman Aerospace Corporation, Bethpage, New York

Computational aerodynamic methods have had a dramatic effect on aircraft design Computer flow simulations have, to a large extent, replaced the wind tunnel as the aerodynamicist's primary design tool This paper describes the aerodynamic design of a family of advanced airfoil shapes suitable for the blade of a new technology general aviation propeller The computational design directly resulted in a successful flight test, eliminating the costly process of tunnel testing The requirements and constraints imposed on the new airfoils are outlined, along with the characteristics of the original propeller airfoils The design approach and procedures are discussed

Nomenclature

C	= speed of sound
C_D C_d	= drag coefficient
CDF	= friction drag coefficient
CDW	= wave drag coefficient
C_L C_l	= lift coefficient
C_M C_m	= pitching moment coefficient (about quarter chord position)
C_p	= pressure coefficient
H	= mapping modulus
L	= lower surface
L/D l/d	= lift to drag ratio
M	= Mach number
$M \times N$	= mesh point density
NCY	= number of flow cycles
Q	= velocity
R	= range
RN Rn	= Reynolds number
S	= physical plane coordinate
TSFC	= thrust specific fuel consumption
t/c	= thickness ratio
U	= upper surface
W	= weight
y/b	= span position
α ALP	= angle of attack
δ^*	= boundary layer displacement thickness
η	= propulsive efficiency
θ	= computational plane coordinate
ϕ	= perturbation velocity potential
Subscripts	
C	= computed
T	= target

Background

AIRCRAFT wing design methods and procedures have advanced significantly over the past 15 years This can be attributed to the development of sophisticated computational methods for use on high speed computers Previously, the wind tunnel served as the primary design tool, but it was expensive and final performance levels were often limited by time constraints due to the large number of variables to be considered Now, both wind tunnel and flight tests are used to verify or check a design that has been derived primarily by computer analyses The performance levels of new aircraft designs attest to the success of this approach The design of the new Gulfstream III provides a good example The Grumman G II, designed in 1966, required 24 different wing shape tests to realize its full performance potential The Grumman designed G III, designed in 1979, required only one wing/winglet test to verify the computer design The G III holds United States to Europe speed and range records

Propeller blade airfoils now in use (Clark Y NACA 16) have existed since World War II While there is considerable incentive from a manufacturing point of view to use these simple shapes, there is also mounting evidence that ap preciable performance gains can be obtained by designing more sophisticated blades Bocci[1] employed an airfoil analysis code in the design of the ARA D family of airfoils These airfoils have been incorporated in "advanced" propeller blade designs and performance benefits have been noted One distinguishing characteristic of these airfoils is the design lift, which is considerably higher than that of past practice. This results in a reduced blade chord for a given disk loading and an attendant reduction in blade weight In ad dition, performance benefits have been identified for climb conditions

Keiter[2] recently underscored the need to improve general aviation propeller technology This would permit compliance with increasing energy conservation needs and environmental requirements The effort described in this paper addresses one facet of improved propeller technology: the application of advanced aerodynamic computational methods to the design of high efficiency propeller airfoils Airfoil lift to-drag ratios are maximized for a given set of requirements and restric tions This increases the propeller aerodynamic efficiency. Design lift coefficients are raised to reduce blade chord length and provide a weight savings No attempt has been made to vary section geometry (camber and thickness) analytically because of the considerable variations in Mach and Reynolds numbers between the blade hub and blade tip Instead, many airfoils are specified to provide the blade designer with sufficient options in designing the blade stack While propeller blade airfoil flows are not strictly two dimensional, it is reasonable to expect that good airfoil characteristics that can be identified by two dimensional analysis will ultimately transfer into good blade characteristics

In 1981, the McCauley Accessory Division of Cessna Aircraft Company initiated this advanced airfoil family design effort Studies are also in progress to identify potential benefits of similar advanced airfoils in relation to Grumman propeller driven aircraft (see Fig 1) The airfoil shapes,

Received July 13 1983; presented as Paper 83 1791 at the AIAA Applied Aerodynamics Conference Danvers Mass July 13 15 1983; revision received April 17 1984

*Associate Engineer Aerodynamics Section. Member AIAA

therefore, cannot be included in this paper because of their proprietary nature.

Discussion

The design of airfoils for propeller applications is a very challenging task because of large variations in Mach and Reynolds numbers along the blade span. In addition, each blade airfoil element must perform well at low lift for cruise conditions and at high lift for takeoff and climb conditions. Many practical constraints must be imposed on the airfoil shape to ensure cost-effective manufacturing and a resultant smooth blade surface. Clearly, there is no computer analysis in existence that can produce an optimum airfoil shape given a large number of aerodynamic requirements and geometric constraints. For this reason, a design procedure and computer codes had to be developed to perform this task in an effective and efficient manner.

Airfoil design methodology and approaches[3] were studied to determine which codes would be applicable. The synthesized shapes would then be analyzed and evaluated using the time-proven Korn-Garabedian Code.[4] Existing airfoils and airfoil families[5-7] were examined to assure that the newly designed airfoils would exceed the performance of any airfoils already available.

Blade Airfoil Design Goals/Constraints

The airfoil section Mach number and Reynolds number values for the current blade were used for setting design flow conditions for the new airfoils. The aerodynamic goals and geometric constraints are itemized below.

Aerodynamic goals: 67% increase in airfoil L/D ratio; good L/D ratio over a wide C_L range; moderate pitching moments (NACA 16 levels $C_M \leq -0.16$); high C_L design point for reduced blade chord; and thick (30%) root airfoils for blade/spinner integration.

Geometric constraints: no upper surface concavity; large leading edge radius (to minimize foreign object damage); gradual lower surface contour; and trailing edge thickness greater than 0.5% chord.

The current propeller blade thickness, Mach number, and Reynolds number distributions are shown in Figs. 2-4, respectively. Based on the airfoil element t/c requirements (Fig. 2) and the expected variation in Mach and Reynolds numbers across the blade span, seven stations were selected for developing primary airfoils. These stations are positioned at the 20, 30, 45, 60, 75, 87, and 100% maximum radius locations.

The new airfoils had to provide a lift-to-drag increment of at least 67% when compared to current technology airfoils. This is a relatively straightforward requirement which will increase the blade aerodynamic efficiency. The airfoils were also required to have good L/D performance over a large range of C_L because the blade operates at high lift for takeoff and climb and at low lift for cruise. NACA 16 series airfoils

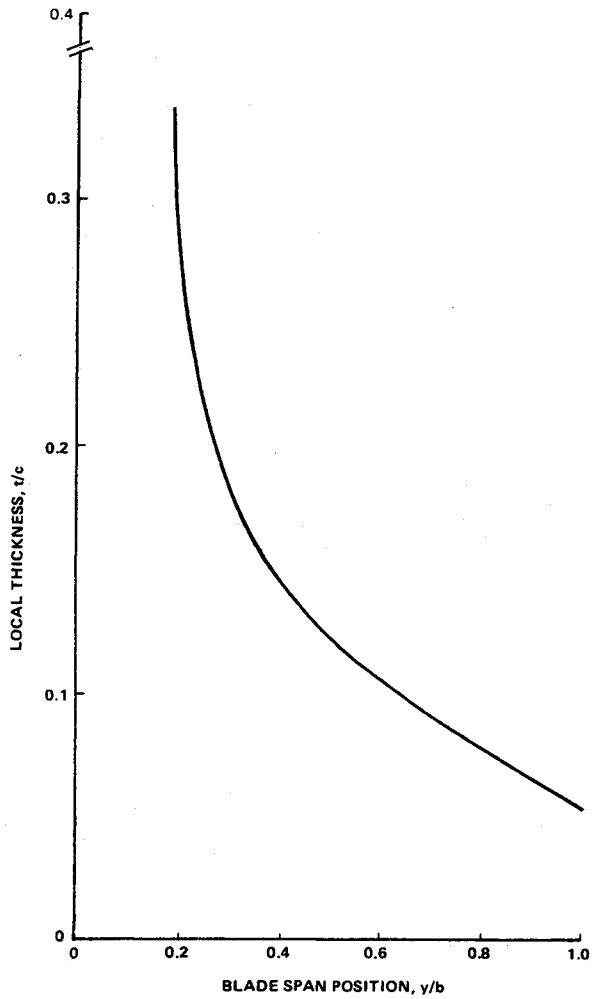

Fig. 2 Propeller blade design—thickness distribution.

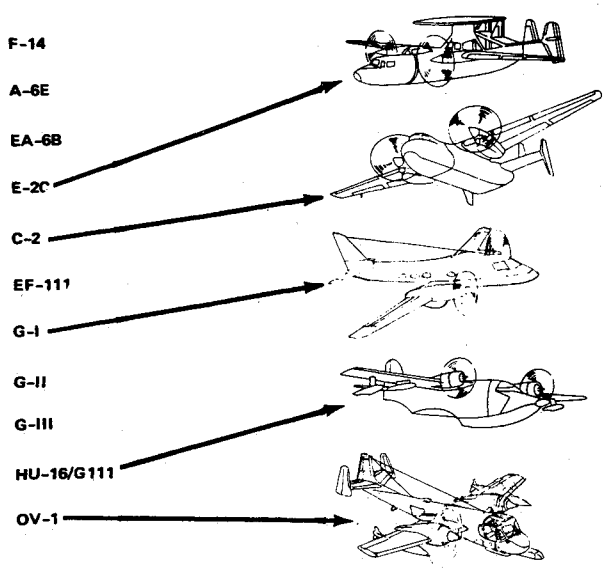

Fig. 1 Current aircraft production modification propeller type.

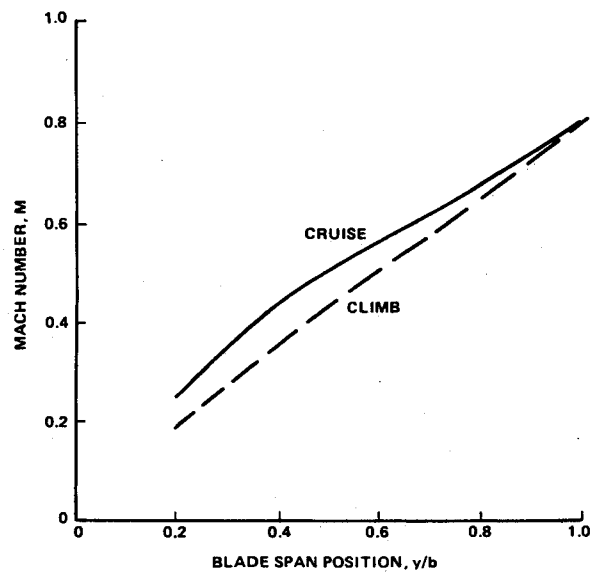

Fig. 3 Original propeller blade operating Mach number.

exhibit good Mach penetration, but the inherent sharp nose shape provides good L/D only for a narrow range of lift To overcome poor low Reynolds number performance, many new propellers are designed using a combination of NACA 16 series and NACA 64 series airfoils The new airfoils should eliminate these restrictions and penalties

Airfoil pitching moments must be constrained to minimize blade stresses and hub structure weight Ideally, the pitching moment for the new airfoils should be consistent with that of NACA 16 series airfoils The moment for any NACA 16 airfoil will depend on both the design lift coefficient and Mach number Moments increase with increases in design lift Since the design lift increases between the propeller blade tip and hub, the moment constraint is less severe as the hub is approached Therefore, the largest moment constraint can be found at the blade tip Both experimental data and numerical analysis have been used to identify the maximum allowable pitching moment at the blade tip station Figure 5 illustrates typical NACA 16 series pitching moment levels [8] To simplify the design process and enhance the probability that the designed airfoils will exhibit a smooth geometric transition between the hub and tip, a constant pitching moment con straint of $C_M = -0\ 16$ was enforced

The cruise and climb lift coefficient distributions for the current propeller blade are shown in Fig 6 In order to in crease the good L/D range, increase L/D_{max}, and reduce blade chord length and weight, the design lift of the new airfoils had to be considerably higher than those of the original blade This requirement was relaxed only in the root or hub region where attached flow considerations restrict the maximum lift obtainable

Studies have indicated that performance gains can be obtained by carefully integrating the design of the propeller root and spinner One feature of future integrated hub designs will be the extension of thick (~30%) airfoil shapes into the spinner cone These shapes should produce less drag than the circular cross section now in use The design lift coefficient of the thick new airfoil must be sufficiently high, however, to provide an endplating effect for the high lift airfoils out board Unlike the high thrust outboard sections, the inboard airfoil must primarily be designed to minimize trailing edge flow separation

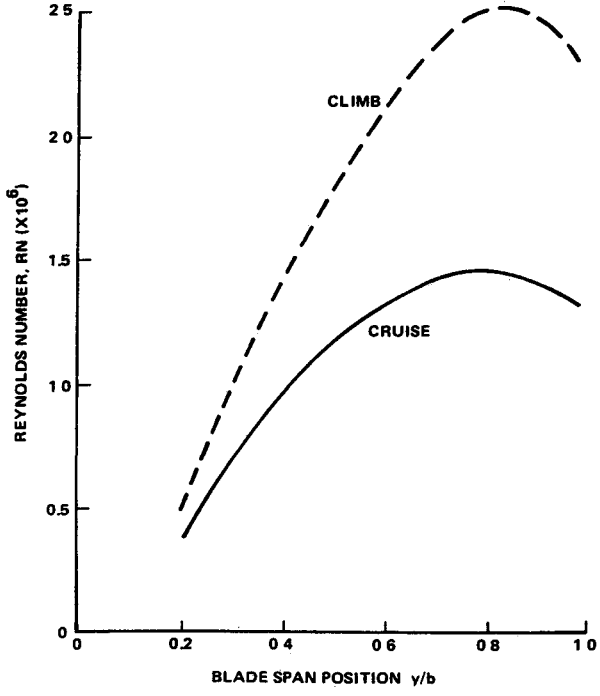

Fig 4 Original propeller blade operating Reynolds number

The preceding discussion has focused on blade design goals and constraints It is also important to identify the constraints or limitations of the computer simulations used for analysis The Korn Garabedian Code has been selected for analyzing the newly designed airfoils This code predicts the airfoil drag levels reasonably well, but care must be taken to note the predicted flow separation point No method currently in existence is capable of predicting drag when appreciable

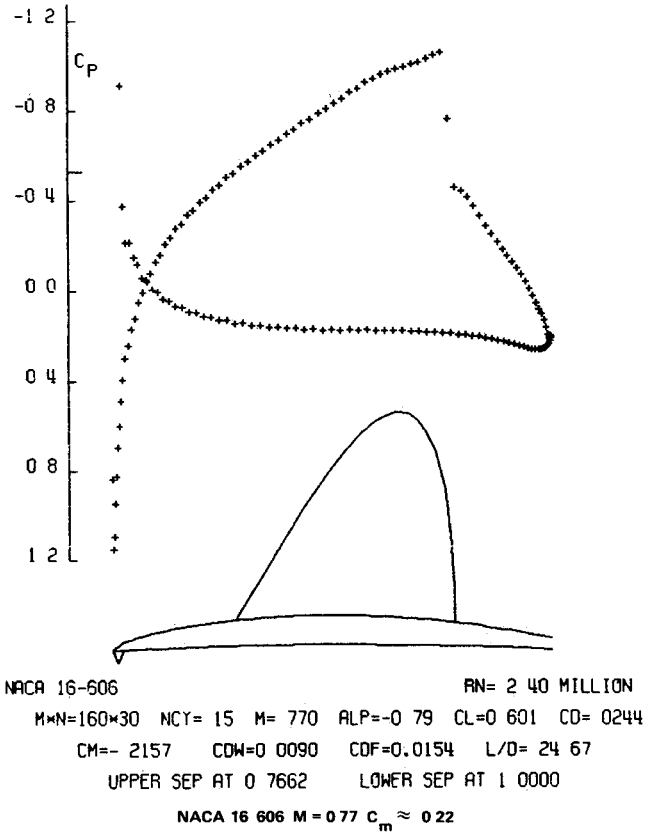

a) Experimental data

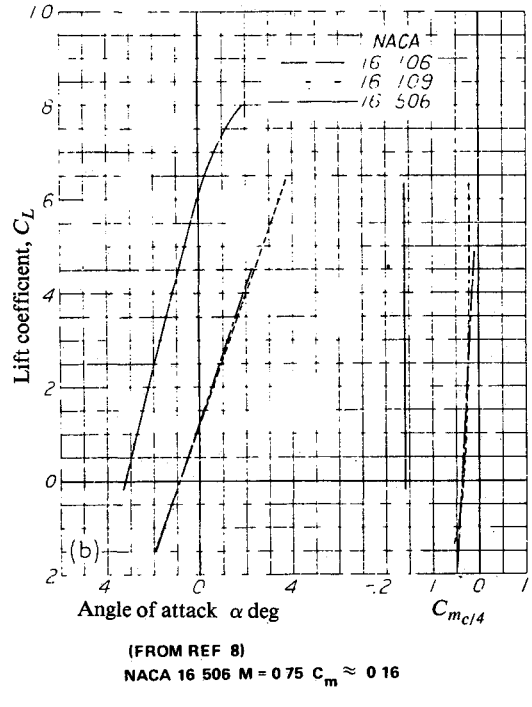

b) Korn analysis

Fig 5 NACA 16 series pitching moment

regions of separated turbulent flow are present If the flow separation point is within certain limits, the predicted drag level is probably realistic Figure 7 illustrates a correlation performed using the NASA GA(W) 1 airfoil. Note that the analytical drag polar compares well with experimental data[9] except in regions where the predicted flow separation point is upstream of the 95% chord location In addition to the airfoil design requirements already identified, it is important to include flow separation points of 95% chord or better as a design requirement Similarly, predicted drag polars should be accurate only in the separated point limited regions Drag predictions outside these regions may be in error by the levels indicated on Fig 7

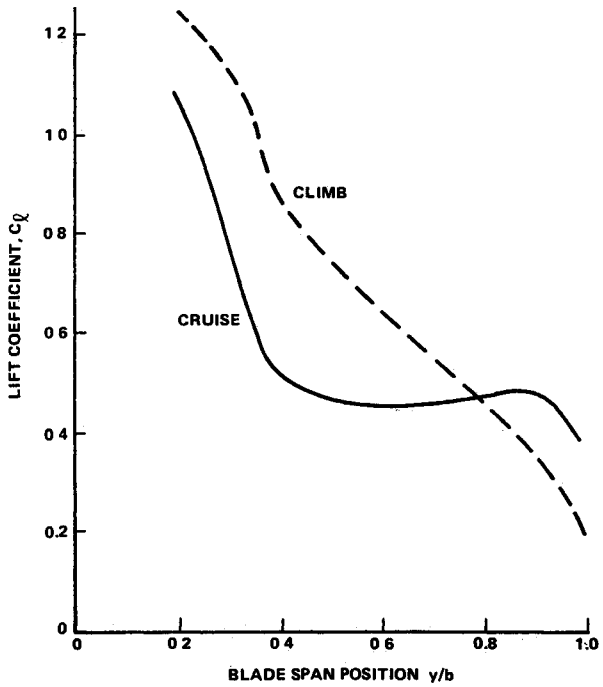

Fig. 6 Original propeller blade operating lift coefficient

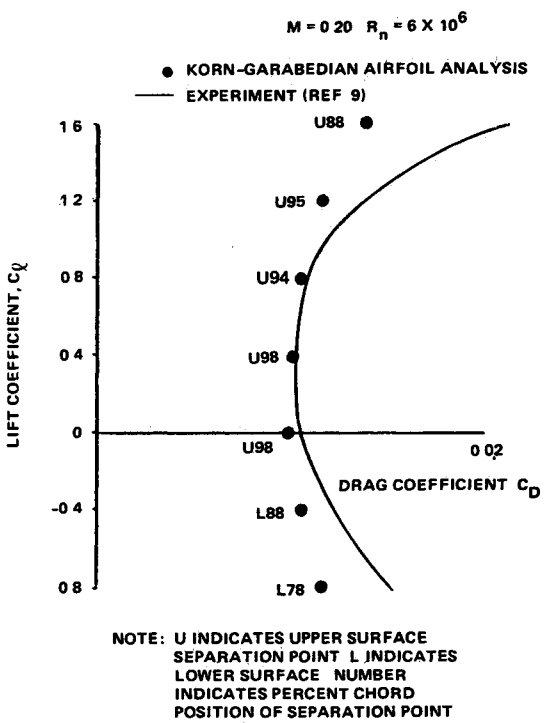

Fig 7 NASA GA(W) 1 airfoil: Effect of flow separation point on predicted drag

Design Methodology

Prior design methods have provided much useful in formation,[3 4 10 14] but restrictions have hindered many ap plications For example, the hodograph method developed during the early 1970s was used to design inviscid shockless airfoils One of the difficulties with the approach is that the

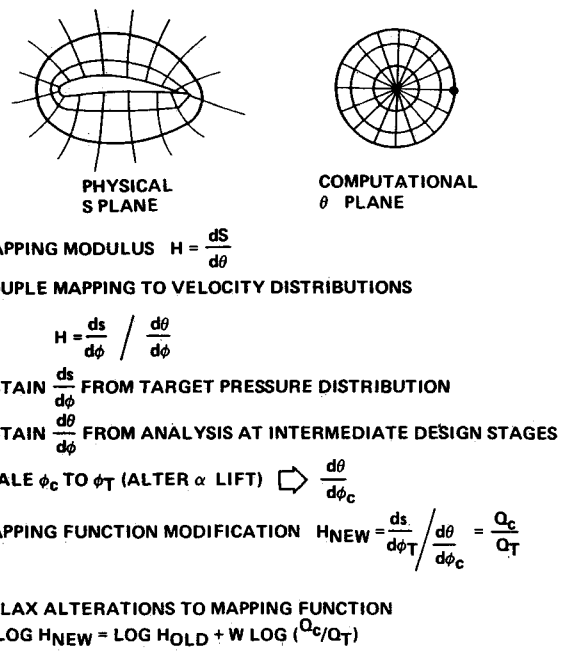

Fig. 8 Modified mapping modulus approach for airfoil synthesis

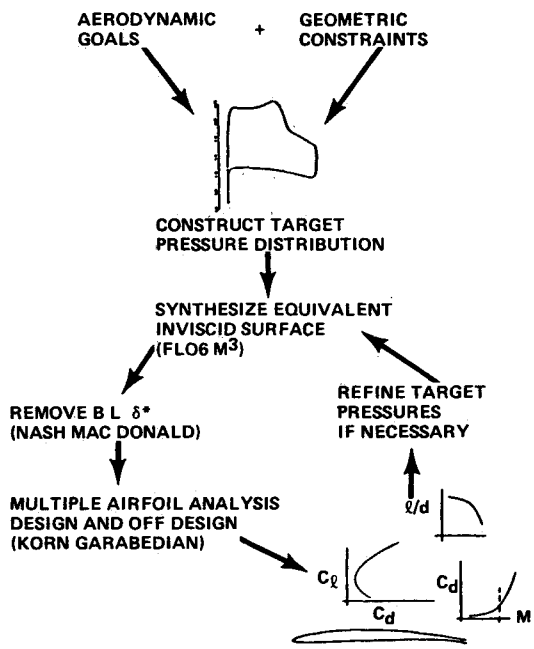

- STRENGTH OF A DIRECT SOLUTION
- DESIGNS ENTIRE AIRFOIL INCLUDING THE LEADING EDGE
- HIGH LEADING EDGE RESOLUTION
- TREATS FLOWS WITH STRONG SHOCK WAVES
- CONTROL OF TRAILING EDGE THICKNESS
- SIMPLE FORMULATION PROVIDING GOOD PHYSICAL FEEL

Fig 9 M^3 automated design process

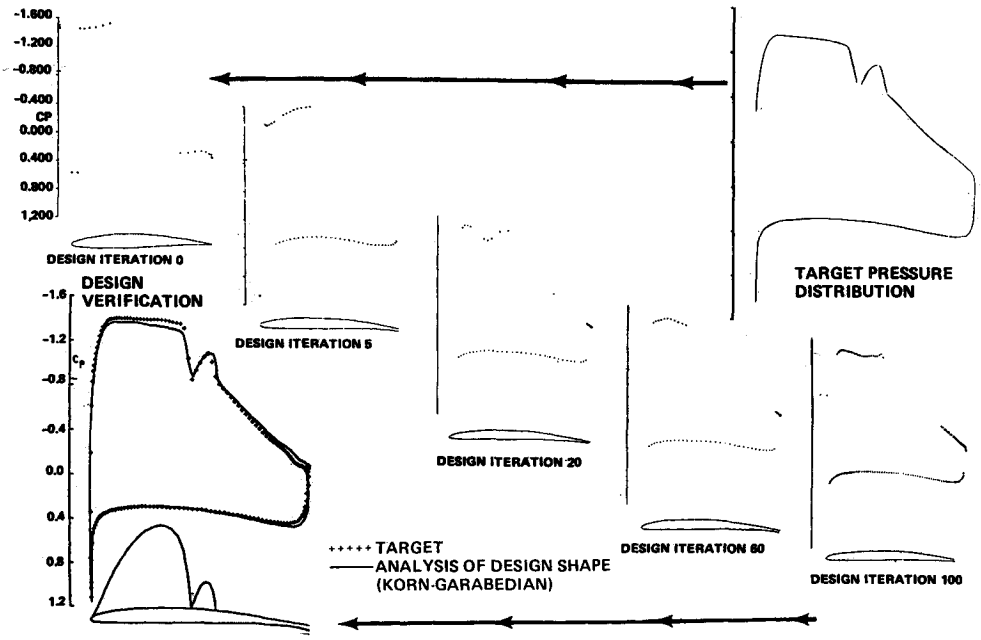

Fig. 10 M^3 iterative-direct airfoil design sequence.

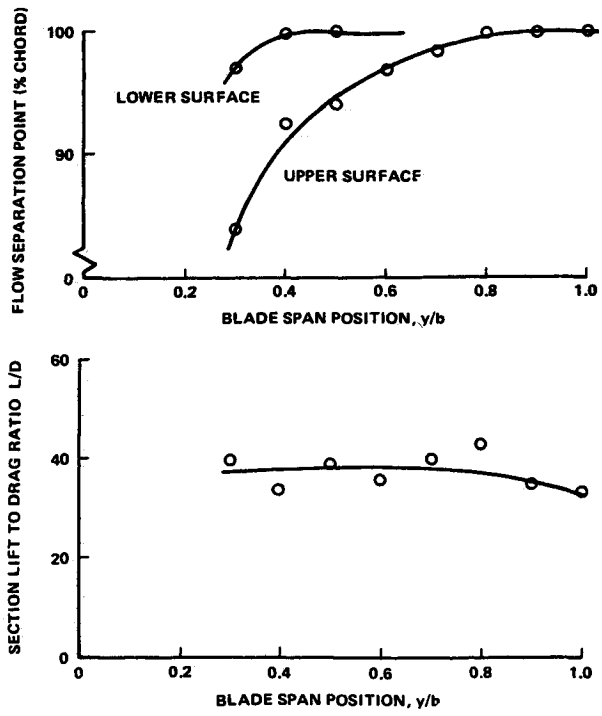

Fig. 11 Original production propeller, Clark-Y airfoil: Korn-Garabedian baseline analysis-cruise condition.

designer is forced to design at flow conditions that differ from those for peak airfoil efficiency To gain a better understanding of this statement, consider the Breguet range equation:

$$R = \frac{C}{\text{TSFC}} M \frac{L}{D} \ln \frac{W_2}{W_1} \tag{1}$$

This equation is suitable for aircraft with jet engines. It can be seen that the range is directly affected by propulsion, structural, and aerodynamic characteristics. For the aerodynamic component, the range will be maximized when the ML/D term is greatest. Typically, this term will be at its peak just beyond the drag divergence Mach number. In other words, taking some purely subsonic point, the Mach number can be increased before drag (derived from shock-wave losses and flow separation) rises to dominate the expression, causing a net reduction in range. At this maximum ML/D condition, the wing or airfoil section will have a "healthy" shock wave present on the upper surface. Similar arguments can be used to explain the presence of strong shock waves during sustained high-speed maneuvers. A shock-free design point, then, would be one for which flight would be relatively inefficient. The airfoil could 1) be made thicker with an attendant reduction in wing weight, 2) operate at higher lift, or 3) operate at higher design Mach number. If any of these options or a combination of these options are implemented, airfoil performance will increase with a relatively strong shock wave forming in the process. Shock-free or subsonic type design techniques then put an added burden on the design engineer since he must determine true airfoil performance at maximum ML/D transonic conditions while the actual high-speed design is performed at less severe flow conditions. To further compound this problem, the hodograph designer must manipulate a set of up to 20 interrelated (and not necessarily physical) variables for each design case. This is more difficult than operations performed to obtain an airfoil surface contour by modifying an airfoil pressure distribution.

The fictitious gas method of Sobieczky[14] is affected by similar constraints. Only shock-free airfoils can be designed. The technique arrives at a shock-free shape by making the airfoil thinner, but this is not always a suitable solution to drag minimization or shock-wave weakening.

The TRANDES method developed by Carlson[13] is constrained to design only the last 85% of the airfoil chord. The first 15% of the airfoil chord must be fixed to provide a starting potential field for the mixed direct-inverse scheme. Unfortunately, many new applications require modifications or refinements to the airfoil leading edge, and existing nose contours are often not suitable for the remainder of the section to be designed specifically for a new set of requirements.

Tranen's method[11] solves the inviscid inverse design problem. This code is restricted in applications since it is not generally possible to specify both the freestream velocity and velocity distribution on the airfoil surface. The method is useful for improving airfoil pressure distributions, but successful cases are limited to those for which small modifications were made to pressure distributions taken from direct solutions. It is important to start with an airfoil that is close to the airfoil being designed.

Table 1 Current production propeller, Clark-Y airfoil: Korn-Garabedian baseline analyses

Blade span position	Thickness, t/c	Cruise, $M/C_L/RN$	Climb, $M/C_L/RN$
0.2	0.337	0.247/1.093/0.376	0.182/1.247/0.498
0.3	0.187	0.353/0.804/0.718	0.269/1.143/0.980
0.4	0.145	0.436/0.522/0.991	0.349/0.860/1.421
0.5	0.122	0.501/0.462/1.188	0.425/0.759/1.804
0.6	0.106	0.560/0.447/1.325	0.499/0.648/2.118
0.7	0.091	0.619/0.453/1.420	0.575/0.549/2.363
0.8	0.078	0.680/0.464/1.468	0.650/0.449/2.517
0.9	0.064	0.747/0.337/1.420	0.727/0.226/2.491
1.0	0.052	0.791/0.386/1.322	0.784/0.231/2.353

Recently, Volpe[15] reported on a nonconservative, inviscid, inverse design code based on a surface mass balance method to modify the airfoil geometry. The new method contains a free parameter that is adjusted during the computation to assure the existence of a solution to the inverse problem.

Davis[16] and McFadden[17] both describe iterative-direct approaches to the airfoil design problem. Direct solutions are sought with an airfoil shape modified iteratively to minimize the difference between the computed pressures and a prescribed target pressure distribution. The existence problem is avoided in this approach because a closed airfoil for a prescribed pressure distribution is not sought.

Grumman's airfoil synthesis methodology is based on the modified mapping modulus (M^3) approach of McFadden. It has been extended by Jameson to include design cases with strong shock waves and further refined by Davis (see Fig. 8). In this formulation, the airfoil mapping modulus

$$H=\frac{dS}{d\theta} \tag{2}$$

is coupled to the velocity distributions

$$H=\frac{dS}{d\phi}\Big/\frac{d\theta}{d\phi} \tag{3}$$

where S is the physical plane coordinate and θ is the computational coordinate. Local values of $dS/d\phi$ are obtained from the target pressure (velocity) distribution. Local values of $d\theta/d\phi$ are obtained from the calculated surface velocity distribution at each iteration. Then ϕ is scaled so that the calculated lift is approximately equal to the target lift by adjusting the angle of attack for each iteration. The mapping modulus modification is then

$$H=\frac{dS}{d\phi_T}\Big/\frac{d\theta}{d\phi_C}=\frac{Q_C}{Q_T} \tag{4}$$

where ϕ is now the integral of Q about the airfoil. The alterations are then "relaxed" into the solution

$$\log H_{\text{new}}=\log H_{\text{old}}+W\log\frac{Q_C}{Q_T} \tag{5}$$

This scheme has been constructed around Jameson's FLO-6[18] nonconservative full-potential equation airfoil code. As a result, it is consistent with the Korn-Garabedian[4] direct analysis method that is commonly used for analysis applications. The implementation scheme has been sketched in Fig. 9. Aerodynamic goals and geometric constraints are combined with the arc length/pressure distribution of an existing airfoil with characteristics that are similar in some respect (i.e., t/c) to the desired airfoil. A target or desired pressure distribution is constructed. The synthesis code (M^3) generates the equivalent inviscid shape required to produce the desired pressure distribution. Note that the equivalent inviscid shape is the total shape that interacts with the freestream flow to generate the flowfield. It includes both the airfoil shape and the boundary layer displacement thickness δ^*. In the next step, the δ^* distribution is computed using the Nash-Macdonald scheme and the upper and lower surface pressure distributions. The δ^* is stripped from the equivalent inviscid shape, leaving the basic airfoil shape. The airfoil is then analyzed using the Korn-Garabedian Code at design and off-design conditions. If the goals and constraints are not satisfied, the target pressures are refined by the designer and the automated design loop is repeated. Note that, with a single computer analysis, the designer can relate a requested pressure distribution to an airfoil shape and all of its aerodynamic characteristics. This is a critical capability when complex requirements are specified.

A typical M^3 iterative-direct sequence is shown for a number of iteration steps in Fig. 10. Computations have shown that the synthesis process is not sensitive to which starter airfoil is used. A moderately thick NACA conventional section has been precanned in the analysis for initiating the sequence. The target pressures and flow condition prescribed are for a thin high-performance supercritical airfoil. The airfoil shape is analyzed for design verification at the end of the sequence; it can be seen that the target pressures agree quite well with the final analysis.

In summary, the M^3 approach is a simple formulation which provides the designer with good physical insight. The entire airfoil, including the leading edge, can be synthesized with high resolution. Flows with strong shock waves can be treated, and control over the airfoil trailing edge closure is possible.

Design Approach and Procedures

In order to establish a baseline for measuring design improvements, nine airfoils from the original propeller blade were constructed for analysis by the Korn-Garabedian Code. Table 1 lists the analysis flow conditions for each section along the blade span.

Figures 11 and 12 provide the spanwise distribution of L/D and flow separation point for the original production propeller airfoils at the cruise and climb conditions, respectively. These distributions will be used to gage the performance benefits of the new airfoils. To have some confidence that performance improvements predicted by the computer analysis will be realized in flight, the new design flow separation points should be at or downstream of the 95% chord location.

To provide a reference point from which to launch the airfoil design study, several airfoil catalogs were examined. Selected airfoils had geometric and aerodynamic characteristics which were judged to be useful for initiating the design process. The airfoil families examined were NASA, NACA, Korn, and Wortmann. Each airfoil exhibited some

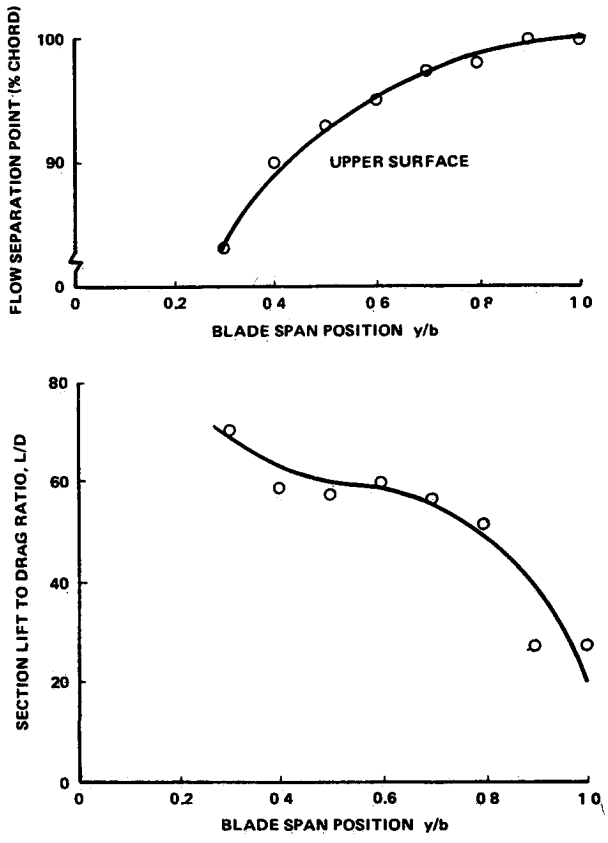

Fig 12 Original production propeller, Clark Y airfoil: Korn Garabedian baseline analysis-climb condition

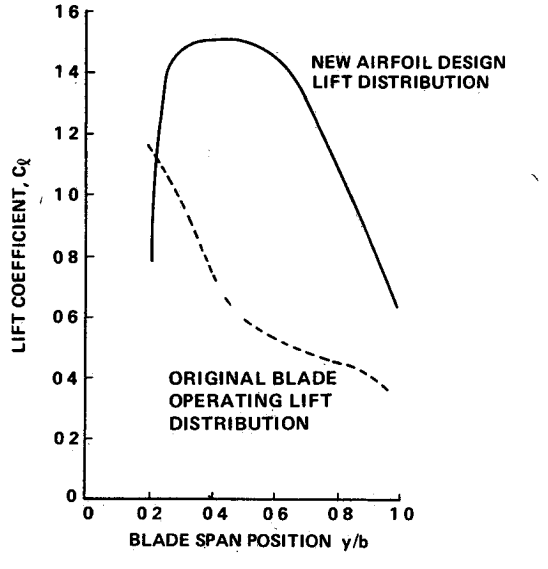

Fig 13 Blade airfoil lift levels

feature which eliminated it from consideration The typical problems were 1) insufficient L/D 2) pitching moment over limit, 3) upper surface concavity, 4) flow separation point too far forward 5) insufficient design lift, 6) narrow lift range for good L/D, 7) small nose radius, 8) insufficient trailing edge thickness, and 9) excessive trailing edge thickness

The minimum trailing edge thickness requirement was 0 5% chord. However, implied in the design of any airfoil is a restriction on the maximum allowable trailing edge thickness To avoid excessive base drag penalties, the trailing edge thickness should not exceed the boundary layer displacement thickness at that point Note that the computer flow

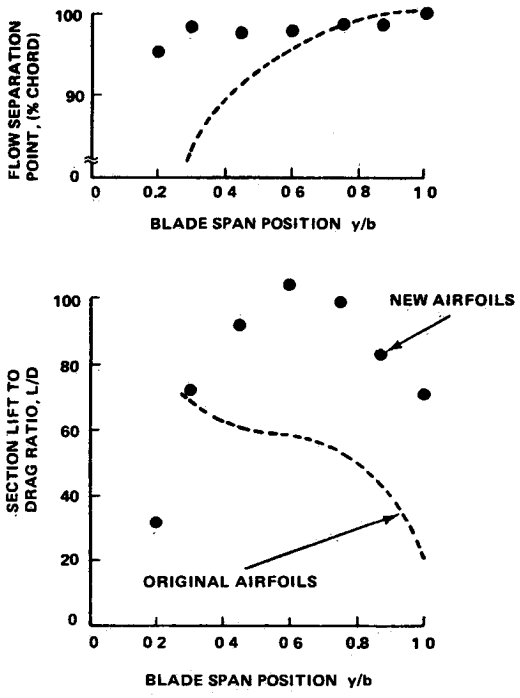

Fig 14 Advanced propeller blade airfoil L/D and flow separation improvement

simulations now in use are not capable of predicting this drag component

While the candidate airfoils just described are not suitable for direct application, their pressure field/arc length relationships provide useful starting points for advanced, tailored airfoils In particular, the Wortmann FX 63 137 airfoil provides a good starting section for the inboard portion of the blade, the design of which is influenced by low speed, low Reynolds number flow separation considerations Friction and flow separation drag must be minimized NASA supercritical airfoils exhibit features that will be beneficial for the outboard portion of the blade, which must be designed to minimize wave drag penalties.

New Design Characteristics and Flight Test

Seven primary airfoils were designed for the nominal 20, 30 45 60, 75, 87, and 100% radius locations The blade designer must have in hand a wide range of airfoils in order to construct the blade airfoil stack A family of sections varying in some simple fashion (i.e , an equation) would serve this purpose, but it is questionable whether the complex requirements of the propeller airfoils could be satisfied if simple relations are implemented Instead, secondary airfoils which offer thickness variations of the primary airfoils were designed The thick secondary airfoils (M 20 and M 30) provide 1% t/c variations The thin secondary sections (M 45 through M 100) provide 0 5% t/c variations Taken together, the primary and secondary shapes yielded 21 different airfoils for the blade design

Supercritical flow development at the 60% span station was identified Shock free flow was achieved at operating lift coefficients that were considerably higher than those of the original propeller The three inboard sections operate at subsonic conditions, while the two outboard sections operate at transonic flow conditions The two airfoils at the 60 and 75% span positions operate in a transition region between the subsonic and transonic flow regions

The new airfoil design lift coefficient distribution is compared in Fig 13 to that of the original blade These high design lift levels permit comparable blade loadings to be obtained with reduced blade chord lengths This provides weight and material savings in addition to reducing the

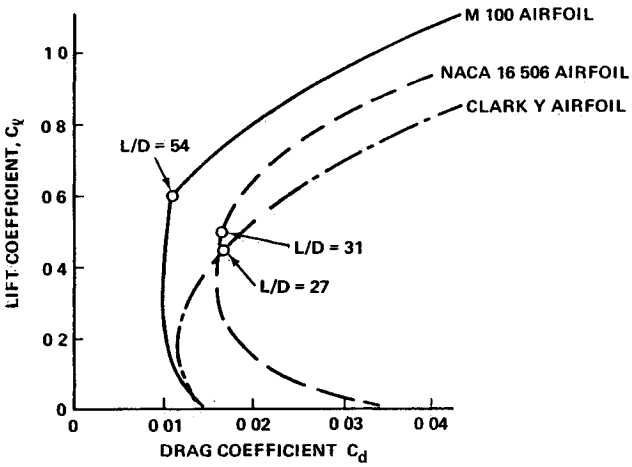

Fig 15 Advanced propeller blade airfoil L/D over a range of lift—100% blade span position

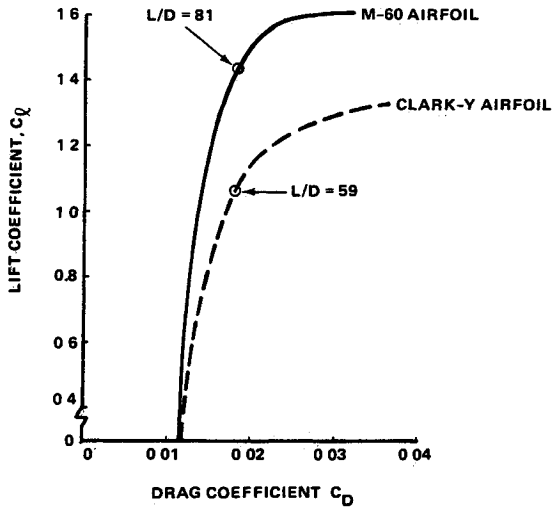

Fig 16 Advanced propeller blade improved L/D over a range of lift—60% blade span position

acoustic disturbance Performance is enhanced by the higher airfoil L/D ratios achieved, as well as by the flow separation improvement Figure 14 illustrates these gains Note that, for the outboard half of the blade (which has the greatest impact on propeller efficiency), the L/D levels exceed the aerodynamic goal of a 67% increment The thick root air foils, which generate little thrust, have been designed for minimum trailing edge flow separation Comparisons for the inboard portion of the blade cannot be made since the original propeller blade airfoils feature separation points which make drag prediction difficult The good L/D operating range of these new airfoils is considerably wider than that of the conventional airfoils This can be seen for the airfoil at the blade tip (Fig 15) and the 60% blade span position (Fig 16) The improved high L/D operating range assures performance gains for both cruise and climb conditions

McCauley designed a propeller blade airfoil stack using these airfoils The blade was fight tested on a Mooney 201 aircraft (see Fig 17) A 1% efficiency gain was identified during climb along with a 2% efficiency gain at (20,000 ft) cruise Blade weight and chord were reduced by one third Blade loading was maintained by high airfoil design lift coefficients The acoustic disturbance was reduced by approximately 1 dB(A) This has been attributed to the reduced blade activity factor smaller flow separation regions, and lack of shock waves The lower blade activity factor also

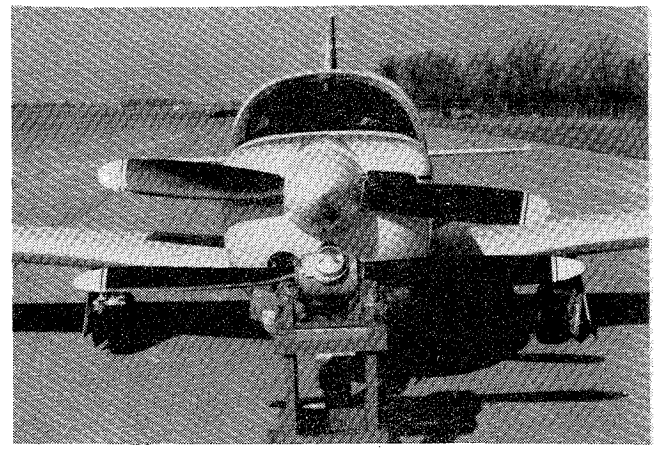

Fig 17 Cessna/Grumman advanced general aviation propeller

reduced static thrust, but this was not judged to be a serious deficiency

Concluding Remarks

1) The application of an airfoil design code to a propeller blade design has been successfully demonstrated

2) Performance benefits in both cruise and climb have been obtained

3) Future designs will feature blunt base sections to take advantage of the base drag/separation drag tradeoff

4) A propeller blade progressed from a computational design to a successful flight test without the need for wind tunnel testing or iterative design test cycles

Acknowledgments

The author would like to acknowledge Charles W Boppe, Aerodynamics Technical Specialist, Grumman Aerospace Corporation for his continuous assistance and guidance in this task Thanks are also extended to Dr Warren H Davis Jr , Senior Engineer, Grumman Aerospace Corporation, for his support

References

[1] Bocci, A J A New Series of Aerofoil Sections Suitable For Aircraft Propellers *Aeronautical Quarterly* Vol 28, Pt I Feb 1977, pp 59 73.

[2] Keiter, I D Impact of Advanced Propeller Technology on Aircraft/Mission Characteristics of Several General Aviation Air craft SAE Paper 81 0584, April 1981

[3] *Advanced Technology Airfoil Research Conference Proceedings* NASA CP 2045, March 1978

[4] Bauer, F Garabedian, P Korn D and Jameson A , *Supercritical Wing Sections II Lecture Notes in Economics and Mathematical Systems* Vol 108 Springer-Verlag New York 1975

[5] Harris C NASA Langley Research Center Hampton Va Private Communication, 1981

[6] Abbott I H and Von Doenhoff, A E *Theory of Wing Sections Including a Summary of Airfoil Data* Dover New York 1959

[7] Althaus D and Wortmann F X *Stuttgarter Profilkatalog I* Friedr Vieweg and Sohn Braunschweig 1981

[8] Stack J. Tests of Airfoils Designed to Delay the Compressibility Bubble NACA TN 976 1944

[9] McGhee R J and Beasley, W D , Low Speed Aerodynamic Characteristics of a 17 Percent Thick Airfoil Section Designed for General Aviation Applications, ' NASA TN D 7428, Dec 1973

[10] Bauer, F Garabedian P and Korn, D , *Supercritical Wing Sections Lecture Notes in Economics and Mathematical Systems* Vol 66 Springer Verlag New York 1972

[11] Tranen T L A Rapid Computer Aided Transonic Airfoil Design Method AIAA Paper 74 501, Palo Alto, Calif , June 1974

[12] Carlson L A Transonic Airfoil Analysis and Design Using Cartesian Coordinates *Journal of Aircraft* Vol 13 May 1976 pp 349 356

[13] Carlson L A , TRANDES: A Fortran Program for Transonic Airfoil Analysis or Design NASA CR 2821 June 1977

[14] Sobieczky H Yu, N J Fung, K Y and Seebass A. R New Method for Designing Shock Free Transonic Configurations *AIAA Journal* Vol 17 July 1979 pp 722 729

[15] Volpe G and Melnik R. E The Role of Constraints in the Inverse Design Problem for Transonic Airfoils ' AIAA Paper 81 1233 June 1981

[16] Davis W H Jr Technique for Developing Design Tools from the Analysis Method of Computational Aerodynamics *AIAA Journal*, Vol 18 Sept 1980 pp 1080 1087

[17] McFadden G B 'An Artificial Viscosity Method for the Design of Supercritical Airfoils R&D Rept C00 3077 158, Courant Mathematics and Computing Laboratory New York University N Y , 1979

[18] Jameson A Iterative Solution of Transonic Flow Over Air foils and Wings Including Flows at Mach 1 *Communications on Pure and Applied Mathematics* Vol. 27 May 1974 pp 283 309